

# Deformation Behavior of Polypropylene/Polyamide Blends

JOACHIM RÖSCH and ROLF MÜLHAUPT\*

Freiburger Materialforschungszentrum und Institut für Makromolekulare Chemie, Stefan-Meier-Strasse 31, D-79104 Freiburg i. Br., Germany

## SYNOPSIS

In recent years, blend technologies have been developed to modify mechanical properties of polypropylene by dispersing discrete stress-concentrating polyamide microparticles in the continuous polypropylene matrix. The work presented here is concerned with the examination of fundamental relationships between blend morphologies and mechanical properties, especially plastic deformation mechanisms at high strain. Polyamide-6, polyamide-12, polyamide-12 plasticized with *N*-butyl-phenylsulfonamide, and polyamide-6 *in situ* embedded in a shell composed of polyamide-36,6 have been used as blend components in polypropylene blends containing 30 vol % of these polyamides. For modification of interfacial adhesion, maleic-anhydride-grafted-polypropylene has been added. When the yield stresses of polyamide and polypropylene are matched, large elongations at break of the resulting blends can be achieved. The influence of crazing, voiding, and shear yielding has been elucidated by transmission electron microscopic analysis of strained blend samples. © 1995 John Wiley & Sons, Inc.

## INTRODUCTION

Unusual property synergisms can be achieved when immiscible polymers are blended together to form two-phase polymer systems where discrete polymer microparticles are dispersed in the continuous polymer matrix of the blend component, which is added in excess.<sup>1</sup> Besides the viscosity ratio of the blend components and processing conditions, the most important parameters governing mechanical failure are size, size distribution, shape, interfacial adhesion, and connectivity of the dispersed polymer microparticles. For toughness enhancement, energy at the crack tip must be dissipated and premature breakdown of voids and crazes, which initiate cracks, must be prevented. One of the important objectives in the development of multiphase polymers is to explore new approaches to preserve high-yield stress without plasticizing the polymer matrix, and to enhance simultaneously stiffness and toughness without sacrificing glass transition temperature of the polymer matrix. In principle, two classes of blends

have been investigated extensively, i.e., rubber-toughened thermoplastics containing dispersed rubber microparticles, and reinforced thermoplastics containing dispersed isotropic or anisotropic rigid microphases, e.g., inorganic fillers, fibers, or other high-modulus polymers, respectively. Due to different thermal expansion coefficients and surface tensions, both types of dispersed microphases are efficient stress concentrators that markedly affect deformation and fracture behavior of such multiphase polymers.<sup>2</sup> Depending on the predominant modes of matrix deformation and failure, e.g., crazing or shear yielding, several deformation mechanisms involving the microparticles can influence resistance against both fracture stresses and crack propagation. In two-phase thermoplastic blends, large deformations cause delamination and voiding at the interfacial boundaries of the dispersed microparticles, especially when interfacial adhesion is poor.<sup>3</sup> For tightly adhering dispersed microphases, such localized crazing and yielding processes involve a much larger volume in comparison to a few isolated crazes formed near the crack tip of a single-phase polymer. As a consequence, such multiple-deformation mechanisms can afford effective energy dissipation near the crack tip and improve impact resistance.

\* To whom correspondence should be addressed.

However, when the modulus and yield stress of the dispersed phase is much higher with respect to the matrix, small strains may be sufficient to initiate crack propagation, e.g., by voiding initiated by dewetting.<sup>4</sup> Therefore, reinforced polymers, e.g., polypropylene containing dispersed polyamide-6,<sup>5-8</sup> exhibit much smaller elongations at break when compared to the pure matrix polymers. Similarly, fillers give higher stiffness at the expense of toughness and elongation at break.<sup>9</sup> In contrast to stiff dispersed microphases, dispersed rubbers, which exhibit much lower yield stresses and moduli with respect to those of the matrix, multiple-deformation mechanisms are much more effective and account for efficient energy dissipation and prevention of unstable crack growth.<sup>10</sup> Moreover, cavitation of the rubber particles can also contribute to energy dissipation. For both rubber-modified<sup>11</sup> and particle-filled<sup>12</sup> thermoplastics, the stress-concentrating dispersed phases appear to promote the formation of shear bands. Although the commercially attractive multiphase polymers containing either rigid or rubbery dispersed microphase have been studied extensively, much less is known about the deformation behavior of multiphase polymers where matrix and dispersed phase exhibit similar yield stresses or moduli. The purpose of this research has been to investigate polypropylene blends where the yield stresses and moduli of dispersed polyamides are varied over a wide range with respect to those of the polypropylene matrix. Yet another objective has been to elucidate the influence of dispersed microphases on shear yielding and cold drawing of the polypropylene matrix and to achieve better understanding of basic structure-property relationships of multiphase polypropylene materials.

## EXPERIMENTAL

### Materials

All polymers were commercially available and used without further purification: polypropylene (Hostalen<sup>®</sup> PPN 1060) from Hoechst AG, maleic-anhydride-grafted-polypropylene (Exxelor<sup>®</sup> PO 2011) from Exxon Chemicals, polyamide-6 (Sniamid<sup>®</sup> ASN27) from Snia, polyamide-12 (Vestamid<sup>®</sup> L1901) from Hüls, polyamide-12 plasticized with *N*-butyl-phenylsulfonamide (Vestamid<sup>®</sup> L2121) from Hüls, hot melt grade polyamide-36,6 derived from dimer acid and hexane-1,6-diamine (Macromelt<sup>®</sup> 6240) from Henkel KGaA. Prior to use the polyamides were dried for the duration of 6 h at 80°C under oil pump vacuum.

### Blend Preparation and Characterization

All blend samples were prepared under identical melt-blending and molding conditions using a Haake Rheomix equipped with a double-screw blender of 60 mL volume. Temperature and torque were measured and controlled simultaneously. After preheating at 240°C, the blender was charged with 40 g of the polymer blend components, as listed in Table I, including 0.2 g stabilizer (80 wt % Irganox 1010 and 20 wt % Irgafos 168, supplied by Ciba-Geigy AG, Basel). Melt blending was performed for 4 min at 60 rpm to prevent thermal degradation. Then the blend was quickly removed and quenched between water-cooled metal plates. Sheets of 1.5 mm thickness were prepared by annealing 10 min at 260°C and compression molding under vacuum using a Schwabenthan Polystat 100 press. Again, the compression-molded sheets were quenched as described above. For tensile testing and determination of Young's modulus, yield stress, and elongation at break, dumbbell-shaped bars were cut and machined following standard procedures described by DIN 53455. Stress-strain tests were performed on an Instron 4204 at 10 mm/min crosshead speed and 23°C. Notched Charpy impact strength was determined according to DIN53453 using 5 test specimen. Morphological studies of blends before and after straining were carried out using the Zeiss CEM902 transmission electron microscope (TEM). Thin sections of 80 to 100 nm thickness suitable for TEM analysis were cut using a Reichert Ultracut E microtoming device equipped with diamond knife. Preferably, for TEM analyses, the blend samples were stained and hardened in ruthenium tetroxide vapors for the duration of 6 h.

## RESULTS AND DISCUSSION

For evaluation of deformation behavior, three types of two-phase polypropylene blends containing 30 vol % of polyamide were prepared by melt blending at 240°C. First, polypropylene (PP) was blended together with polyamide-12 (PA-12) in the presence of 0 to 10 vol % of maleic-anhydride-grafted-polypropylene (PP-*g*-MA) as blend compatibilizer. During processing the pendant succinic anhydride groups of PP-*g*-MA can react with PA-12 amine endgroups to form PP-*graft*-PA-*graft*-copolymers, which covalently couple polypropylene and polyamide via imide groups. Such graft copolymers are known to be efficient dispersing agents and adhesion promoters. Second, in order to identify the role of

**Table I** Composition and Properties of Polypropylene Blends and Blend Components<sup>a</sup>

PP (vol %)	PP-g-MA (vol %)	PA-12 (vol %)	PA-12p (vol %)	PA-6 (vol %)	PA-36,6 (vol %)	PA Domain Size ( $\mu\text{m}$ )	Young's Modulus (MPa)	Yield Stress (MPa)	Elong. at Break (%)	Notched Charpy Impact Str. ( $\text{kJm}^{-2}$ )
100	—	—	—	—	—	—	1100	32	700	6
—	100	—	—	—	—	—	1100	33	500	4
—	—	100	—	—	—	—	1500	50	230	19
—	—	—	100	—	—	—	1000	30	270	24
—	—	—	100	—	—	—	1700	55	00	n.f. <sup>b</sup>
—	—	—	—	—	100	—	130	5	320	n.d. <sup>c</sup>
70	—	30	—	—	—	5.0	1230	27	200	3
68.25	1.25	30	—	—	—	2.5	1250	33	30	7
67.50	2.50	30	—	—	—	1.8	1240	32	35	8
65.00	5.00	30	—	—	—	1.0	1250	32	40	8
60.00	10.00	30	—	—	—	0.7	1230	33	50	9
67.50	2.50	—	30	—	—	1.8	1100	32	500	12
65.00	5.00	—	30	—	—	0.9	1100	32	500	14
60.00	10.00	—	30	—	—	0.6	1100	32	500	14
70	—	—	—	30	—	30	—	23	50	3.5
65	5.00	—	—	30	—	2.5	—	34	25	7
65	5.00	—	—	28.7	1.3	2.9	—	31.5	140	12
65	5.00	—	—	27.5	2.5	3.5	—	31	100	10
65	5.00	—	—	25	5.0	4.5	—	30	75	12

<sup>a</sup> PP: polypropylene; PP-g-MA: maleic-anhydride-grafted PP; PA-12: polyamide 12; PA-12p: PA-12 plasticized with *N*-butyl-phenylsulfonamide; PA-6: polyamide 6; PA-36-6: polyamide-36,6 derived from dimer acid and hexane-1,6-diamine.

<sup>b</sup> n.f.: no failure.

<sup>c</sup> n.d.: not determined.

the yield stress difference between continuous and dispersed phases, the polyamide-12 blend component was plasticized with *N*-butyl-phenylsulfonamide to match yield stresses of polyamide-12 and polypropylene by lowering PA-12 yield stress. The plasticized PA-12 (Vestamid<sup>®</sup> L1901) is abbreviated as PA-12p. Third, polypropylene blends containing dispersed core/shell microparticles with a polyamide-6 core and a soft polyamide-36,6 shell were obtained by simultaneously blending polypropylene together with polyamide-6 and various amounts of a flexible polyamide derived from dimer fatty acid and 1,6-hexanediamine (PA-36,6) in the presence of PP-g-MA compatibilizer. Due to the surface tension gradient of the four blend components, PA-36,6 accumulated at the interface between polypropylene and polyamide-6, thus forming a flexible interlayer with low yield stress and Young's modulus. Average domain sizes of the dispersed PA microphases, as determined by transmission electron microscopic (TEM) imaging, and mechanical properties of the three blend types are listed in Table I.

In the first blend type, similar to other polypropylene/polyamide blends, both PA dispersion, ex-

pressed by the average PA-12 domain size, and interfacial adhesion, which is reflected by blend yield stresses, were controlled by adding maleic-anhydride-grafted-polypropylene (PP-g-MA) as blend compatibilizer. As the PP-g-MA volume fraction increased from 0 to 10 vol %, the average PA-12 domain size was lowered from 5 to 0.7  $\mu\text{m}$ , whereas blend yield stresses were raised from 27 to 33 MPa. In the absence and presence of PP-g-MA compatibilizers, PA-12 gives much smaller PA domain sizes when compared to those of PA-6. This reflects the better compatibility of PA12 vs. PA-6 with respect to the PP matrix. Figure 1 depicts the typical TEM image of a PP/PA-12 blend sample compatibilized with 10 vol % PP-g-MA and strained to 50% elongation. Clearly, the spherical PA-12 domains, which exhibit yield stresses of 50 MPa with respect to 33 MPa of PP, did not change their shape as a result of the applied mechanical stresses. The dark lines, originating at the interfacial regions of the dispersed PA-12 and oriented perpendicular to the external mechanical stresses, could correspond to crazes that were stained preferentially by ruthenium tetroxide vapors. Both experimental observations indicate



**Figure 1** TEM image of PP/PA-12 (70 : 30) strained to 50% elongation.

that dispersed PA-12 microphases did not contribute to plastic deformation but acted merely as stress concentrators. Because PP-*g*-MA compatibilizers gave much enhanced interfacial adhesion, dewetting, microvoiding, and subsequent yielding did not take place. Instead, microcracks, which were initiated at the phase boundaries, appeared to relieve stress concentrations and led to failure shortly after the yield point was reached. As a consequence, the compatibilized PP/PA-12 gave much lower elongation at break. Although TEM analysis of the more fragile thin sections of noncompatibilized PP/PA-12 was not possible, the occurrence of intense stress whitening and cold drawing during straining provided evidence for voiding around PA-12 domains. The difference in interfacial adhesion could account for the much larger elongation at break found in the absence of PP-*g*-MA compatibilizer.

The presence of the PP-*g*-MA compatibilizer, which was varied between 1.25 and 10 vol %, did not influence Young's modulus of 1,240 MPa and yield stress of 32 MPa. Obviously, good interfacial adhesion was achieved at low compatibilizer content,

and the matrix reinforcement was determined by the volume fraction of PA-12, which remained constant. Figure 2 depicts typical stress-strain curves for the three blend types. Noncompatibilized PP/PA-12 blends exhibited weak yield points and started to yield at much lower stress in comparison to PP-*g*-MA-compatible blend. This behavior originated from dewetting and microvoiding of PA-12, which involved the total sample volume. When interfacial adhesion was enhanced by adding PP-*g*-MA, yield stresses increased, but the tightly adhering PA-12 microphases prevented extensive shear yielding of the PP matrix. Both elongation at break of 200% of the compatibilized PP/PA-12 and 50% of the corresponding compatibilized blend are much lower with respect to 700% of the PP matrix. It is a well-known phenomenon of particulate-filled thermoplastics that, in spite of shear yielding, dispersion of filler particles can substantially reduce elongation at break.<sup>13</sup> One explanation for such deformation behavior is that not the total sample volume but only ligaments between adjacent voids are involved in cold drawing of PP. Moreover, when interfacial adhesion is improved, yielding is impeded because craze formation initiates cracks and promotes premature crack propagation.

Because crazing involving the total volume represents an efficient energy dissipating process, it was not surprising that 2.5 vol % PP-*g*-MA compatibilizer gave threefold higher notched Charpy impact strength. Additional PP-*g*-MA did not further improve impact resistance. Interestingly, the threefold increase of notched Charpy impact strength was accompanied by substantially lower elongation at break. There was no correlation found between notched Charpy impact strength and elongation at break or the related area of the stress-strain curve,

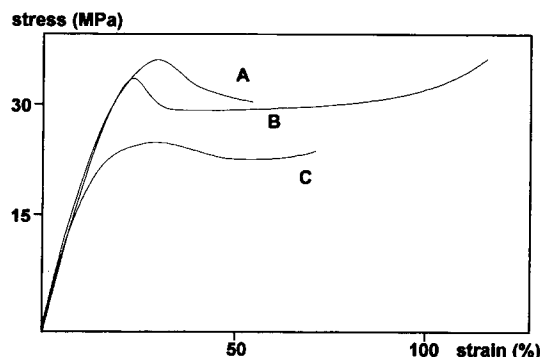


**Figure 2** Stress-strain curves of the PP/PA-12 (70 : 30) blends: PP/PA-12 compatibilized with 10 vol % PP-*g*-MA (A), PP/PA-12p plasticized with *N*-butyl-phenylsulfonamide (B), and noncompatibilized PP/PA-12 (C).

respectively. Obviously, impact resistance is primarily affected by deformation modes and deformation rates. Although poor interfacial adhesion favors voiding and shear yielding during tensile testing at comparatively slow strain rates, it facilitates rapid crack propagation during impact because cracks are readily initiated and propagated at nonadhering PA-12 interfaces. At major deformation, switching from shear yielding combined with voiding to crazing by enhancing interfacial adhesion mode could account for improved energy dissipation and, consequently, much higher toughness.

The first PP/PA-12 blend type was characterized by the presence of adhering or nonadhering rigid PA-12 microparticles that did not undergo mechanical deformation. In order to match the yield stresses of continuous PP matrix and dispersed PA-12 and to induce PA-12 deformation, the second blend type was composed of 70 vol % PP and 30 vol % PA-12 plasticized with *N*-butyl-phenylsulfonamide (PA-12p). This PA-12p exhibited yield stress of 30 MPa, resembling PP yield stress of 32 MPa. Although Young's modulus was slightly reduced from 1,240 to 1,100 MPa, as expected for the lower modulus of the dispersed PA-12p, elongation at break and notched Charpy impact strength were much higher than those of the compatibilized and noncompatibilized PP/PA-12 blends. In spite of the two-phase morphology, the resulting PP/PA-12p blend behaved like a single-phase alloy of miscible blend components. Hence, polymer properties such as Young's modulus, yield stress, and elongation at break of the PP/PA-12p blend were very similar to those calculated from the properties of the individual blend components according to the 70 : 30 mixing ratio. Only the notched Charpy impact strength of 14 kJ/m<sup>2</sup> was slightly higher than that of 11.4 kJ/m<sup>2</sup> calculated for PP/PA-12p (70 : 30). The origins of this unexpected behavior is apparent in Figure 3, depicting TEM image of PP/PA-12p 300% elongation. Upon exposure to mechanical stresses, the dispersed spherical PA-12p gave plastic deformation to produce strained elliptic microphases. As a consequence of similar deformation of both dispersed and continuous phases, the resulting blend reflected the properties of both blend components, as expected from the rule of mixing. Moreover, the stress-strain curve of PP/PA-12p in Figure 2 was nearly identical to that of pure PP.

In the third blend system, the dispersed polyamide microphase was composed of rigid PA-6 with yield stress of 55 MPa, encapsulated in a flexible shell of PA-36,6, which was derived from dimer fatty acid and 1,6-hexamethylene diamine and exhibited

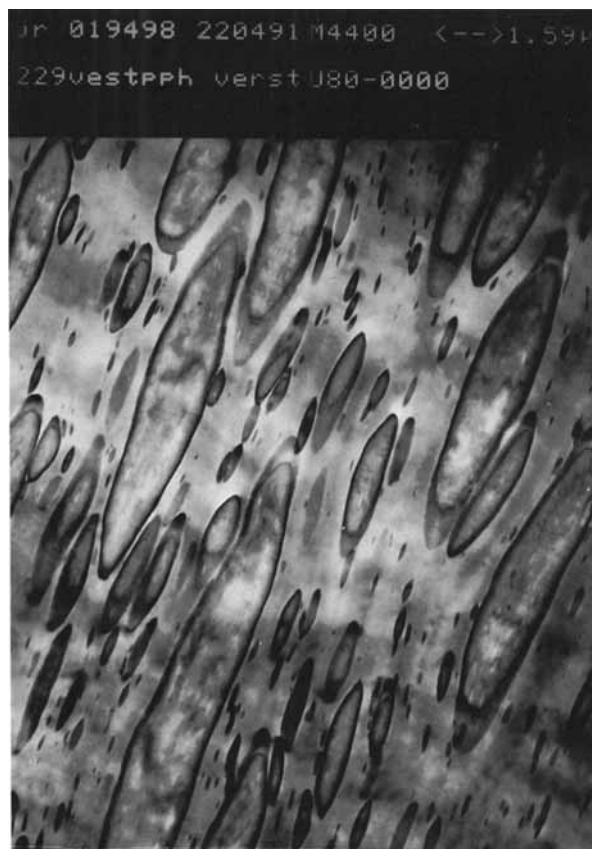


**Figure 3** TEM image of PP/PA-12p (70 : 30) strained to 300% elongation.

Young's modulus of 130 MPa and yield stress of 5 MPa. Figure 4 shows the morphology of such core/shell PP/PA-6/PA-12/PA-36,6 blends. With increasing volume fraction of PA-36,6, equivalent to larger shell thicknesses, yield stress slightly decreased, whereas elongation at break was reduced drastically. High-yield stress indicate good interfacial adhesion, and elongation at break was much higher than that of PP/PA-6. In fact, when compared to PP/PA-6 compatibilized with PP-*g*-MA, the *in situ* formation of PA6/PA-36,6 core/shell microparticles gave much better performance, especially in view of higher notched Charpy impact strength and elongation at break. Small amounts of 1.3 vol % PA-36,6 were sufficient to achieve unusual property synergisms of PP/PA-6 (30 : 70) blends. Because the content of PA-36,6 also affect the average domain size of the dispersed PA-6, it was not possible to apply the model of Matonis and Small<sup>14</sup> to predict optimum shell thicknesses. From Figure 4, it is apparent that the shell is not entirely uniform and does not cover the entire PA-6 surface. When strained to 80%, such a core/shell-multiphase poly-

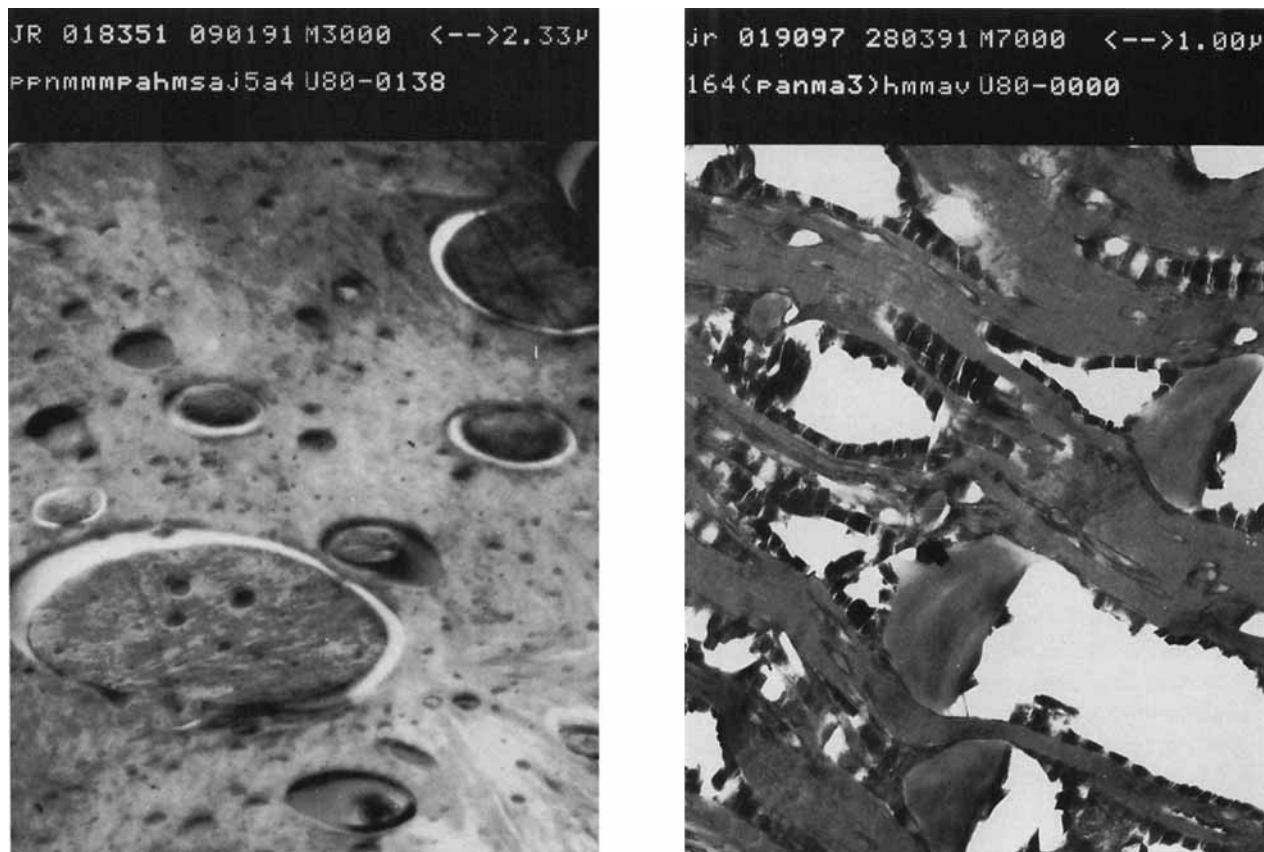


**Figure 4** TEM images of PP/PA-6/PA-36,6 (70 : 25 : 5) before (left) and after straining at 80% elongation (right).

propylene exhibits different deformation behavior. Figure 4 shows the presence of elliptical voids containing spherical PA-6 cores and ruptured shell components. Figure 4, right, where the shell is stained preferentially after rupturing it, shows that the flexible shell was deformed and ruptured, thus generating voids that were expanded during yielding of the PP matrix. Similar to the PP blends containing poorly adhering dispersed phases, voiding resulting from dewetting could account for substantially higher elongation at break. In addition to voiding, plastic deformation and rupture of the flexible shells contribute to energy dissipation and improved impact strength.

## CONCLUSION

The molecular engineering of polymer interfaces in multiphase polypropylene materials represents an attractive route to achieve unusual property synergisms when polypropylene is blended together with other polymers such as polyamide. In the case of

polypropylene/polyamide blends, one can distinguish between two different types: polypropylene containing tightly adhering compatibilized rigid polyamide, e.g., polyamide-6 and polyamide-12, and polypropylene containing discrete microphases of polymers with similar yield stresses such as either plasticized polyamide-12 or rigid polyamide microphases embedded in a flexible thin shell, respectively. In the first case, the dispersed microphases do not take place in plastic deformation but act as stress concentrators. Provided that good interfacial adhesion exists, external mechanical stresses induce crazing at the interfaces before shear yielding of the polypropylene matrix can occur. This accounts for much lower elongation at break of the polypropylene blend with respect to that of polypropylene. At low average domain sizes  $< 1 \mu\text{m}$  of the dispersed polyamides, crazing involving the total sample volume can enhance energy dissipation during impact and promote toughness. In contrast to rigid dispersed phases, plasticized polyamide-12, with yield stresses equivalent to the polypropylene matrix, gives two-phase polypropylene with properties equivalent to

a single phase alloy. Origin of such behavior is the simultaneous plastic deformation of both phases accompanied by extensive yielding. Alternatively, rigid polyamides can be encapsulated in more flexible shells which, in contrast to the rigid core, actively participate in plastic deformation processes and contribute to energy dissipation. Such core/shell-type morphologies can be achieved in blends of polypropylene with polyamide-6 and flexible polyamide-36,6 derived from dimer fatty acid and 1,6-hexanediamine. Due to the surface tension gradient, the more flexible polyamide-36,6 encapsulates the dispersed polyamide-6 during melt processing. Upon straining, the more flexible shell undergoes plastic deformation until voids are formed and the shell is ruptured. These energy-absorbing processes are accompanied by extensive yielding of the polypropylene matrix. As a result of simultaneous plastic deformations and shell cavitation, multiphase polypropylenes can exhibit improved toughness.

## REFERENCES

1. L. A. Utracki, Ed., *Polymer Alloys and Blends*, Hanser Publishers, Munich, 1989.
2. A. J. Kinloch and R. J. Young, Eds., *Fracture Behavior of Polymers*, Elsevier Applied Science, New York, 1983, p. 421.
3. C. B. Bucknall, Ed., *Toughened Plastics*, Applied Science Publishers, Essex, 1977.
4. M. E. J. Dekkers and D. Heikens, *J. Mater. Sci.*, **20**, 3865 (1985).
5. R. Holsti-Miettinen, J. Seppälä, and O. T. Ikkala, *Polym. Eng. Sci.*, **32**(13), 868 (1992).
6. J. Rösch and R. Mülhaupt, *Makromol. Chem., Rapid Commun.*, **14**, 503 (1993).
7. F. Ide and A. Hasegawa, *J. Appl. Polym. Sci.*, **18**, 963 (1974).
8. P. van Gheluwe, B. D. Favis, and J. P. Chalifoux, *J. Mater. Sci.*, **23**, 3910 (1988).
9. W. Bilogan and H. P. Schlumpf, *Kunststoffe*, **70**, 331 (1980).
10. H. H. Kausch, Ed., *Polymer Fracture*, 2nd Ed., Springer, Berlin, 1987.
11. C. B. Bucknall, P. S. Heather, and A. Lazzeri, *J. Mater. Sci.*, **24**, (1989).
12. M. E. J. Dekkers and D. Heikens, *J. Mater. Sci.*, **19**, 3271 (1984).
13. I. L. Dubnikova and V. A. Topolkaev, *Polym. Sci. USSR*, **32**, 782 (1990).
14. V. A. Matonis and N. C. Small, *Polym. Eng. Sci.*, **9**, 90 (1969).

Received March 15, 1994

Accepted January 3, 1995